

Magnetic Cloud Induced Magnetic Storms: A Lack of "Classical" Substorm Expansion Phases

B.T. Tsurutani and X.-Y. Zhou
Jet Propulsion Laboratory
California Institute of Technology, Pasadena, California

W. D. Gonzalez
Instituto Nacional Pesquisas de Espaciais (INPE)
Sao Paulo, Brazil

Submitted to JGR special section "Storm-Substorm Relationship" on 5/10/2001

ABSTRACT

Eleven storms induced by magnetic clouds (occurring in 1997) were studied using WIND interplanetary data and POLAR UV nightside auroral imaging data (magnetic cloud were specifically chosen because the internal magnetic field B_z component typically varies smoothly). For the UV data available, classical substorm expansion phases were detected in only half (5 out of 11) of the storm main phases. In the other 6 events, the storm-time auroras were characterized by longitudinally broad, moderate intensities over the entire nightside oval. The auroras were centered at $\sim 62^\circ$ - 65° geomagnetic latitude, and often with a second band at higher, $\sim 70^\circ$, latitudes. The higher latitude auroras were generally (but not always) confined to the premidnight sector. Dawn and dusk auroras were often more intense than midnight sector auroras. The most prominent auroral forms were north-south aligned patches. These patches extended ~ 1 hr in local time (longitudinal width) by $\sim 5^\circ$ in latitude, and had durations of ~ 3 to 5 min. The auroral patches occurred at all local times in the nightside sector and often attached the two auroral bands in the premidnight sector. Some researchers have ascribed these patches to be the ionospheric manifestations of bursty bulk flows in the plasmashet. Two of the storms occurring without classical substorm expansion phases had interplanetary electric fields > 5 mV/m with durations greater than 3 hrs. The storms peak intensities for these events were $D_{ST} > -100$ nT, even though the interplanetary plasma densities were of average values. One possible explanation is that the presence of classical substorm expansion phases may be necessary for the heating and expulsion of oxygen ions from the ionosphere, and without this added phenomenon, ring current intensities might be substantially diminished.

INTRODUCTION

From the original seminal substorm definition paper (Akasofu, 1964) to more recent reviews on storm-substorm relationships (Kamide et al., 1998), it has been a "common knowledge" that substorms and substorm expansion phases are an integral part of magnetic storm main phases. It has even been stated that all storms studied in the past contain substorms (Kamide et al., 1998). However, the importance of substorms within storms has been not well understood, and it has been and it is currently being debated (McPherron, 1997; Rostoker et al., 1997).

The purpose of this paper will be to examine a specific but important subset of magnetic storms, those that are caused by large southward, smoothly rotating magnetic fields: interplanetary magnetic clouds. Such smooth IMF B_z rotations may not provide the abrupt interplanetary/magnetospheric electric field changes believed to be necessary for substorm expansion phase triggering (Lyons et al., 1997).

METHOD OF ANALYSES

All 11 (fast) magnetic clouds that occurred in 1997 are used in the study. These events are presented in Lepping et al. (2001) and are indicated in Table 1. The WIND plasma and magnetic field data have been used to calculate the solar wind ram pressure and plasma beta. The WIND magnetometer is described in Lepping et al. (1995) and the plasma instrument in Ogilvie et al. (1995). The magnetic cloud intervals are identified using from the plasma beta and the magnetic field characteristics. Beta values < 0.1 and smooth fields are characteristics of clouds (Tsurutani and Gonzalez, 1995). The magnetic field magnitude $|B|$, IMF B_s (peak values of B_s are noted) and solar wind speed V_{sw} shown in the Table are values at the center of the magnetic cloud.

Table 1. 1997 Magnetic Cloud Events

Event	Date (1997)	Cloud Interval (UT)	$ B _{\max}$ (nT)	B_s max (nT)	V_{sw} (km/s)	D_{ST} min (nT)
1	Jan 10-11	0440-2040	15	-15	450	-78
2	Feb 10	0245-1900	9	-7	500	-68
3	Apr 21-23	1205(4/21)-0700(4/23)	15	-10	390	-107
4	May 15-16	0945(5/15)-0100(5/16)	25	-25	450	-115
5	Jun 09	0200-2300	12	-10	360	-84
6	Jul 15-16	0615(7/15)-0100(7/16)	13	-13	350	-45
7	Aug 03-04	1350(8/3)-0100(8/4)	15	-13	450	-49
8	Oct 01-02	1600(10/1)-2300(10/2)	10	0	460	-98
9	Oct 10-12	2300(10/10)-0000(10/12)	13	-10	440	-130
10	Nov 07-08	0530(11/7)-1200(11/8)	15	-13	450	-110
11	Nov 22-23	1850(11/22)-1800(11/23)	25	-15	500	-106

The auroral forms were taken from the POLAR imaging using the LBH Long wavelength filter. The highest time resolution used was ~ 3 min, more than adequate to resolve substorm expansion phases. Due to POLAR orbital restrictions, the entire main phases of each of the magnetic storms were not observed. Only images for parts of each event were available. However, in most cases substantial lengths of time were available (hours), so definitive statements about the detection or lack of detection of classical substorm expansion phases can be made.

Classical substorm expansion phases have been described by Akasofu (1964). Some of the salient features are: 1) a brightening of the equatorward-most arc in 0-5 min; 2) poleward, westward and eastward expansion of auroral forms in 5-10 min; 3) maximum expansion occurs in 10-30 min; and 4) arcs reform and drift back to their quiescent latitudes in 30 min- 1 hr. Akasofu (1964) also mentioned that during interval of strong activity, the substorm expansion

phase (steps 1 through 3) can take place in 5 to 10 min. It will be this classic substorm expansion phase sequence that we will look for during magnetic cloud related storms.

An example of two substorm expansion phases that occurred during a magnetic storm that was associated with a magnetic cloud are shown in Figure 1. The first event is visible at 0839:42 UT. An arrow is placed between that image and the previous image to indicate that the onset occurred somewhere between the two images. The temporal resolution is ~ 6 min. In each image, noon is at the top and dawn at the right. In the 0839:42 UT image, there is a sudden brightening (red color) from 23 LT to 02 LT at latitudes between 60° and 68°. In the next image, at 0845:50 UT, the intense aurora has expanded westward (to 2230 LT), poleward (to 71°), and eastward (to 3:30 LT). The expansion phase is completed by 0851:58 UT, giving a duration of ~ 12 min.

The second substorm expansion phase onset occurs between 0922:38 UT and 0928:46 UT. At 0959:26 UT, the aurora had reached maximum in spatial extent and spans from ~ 21 LT to 03 LT and from 60° to 75° MLT. The duration of this expansion phase is ~ 30 min.

The interplanetary and D_{ST} data for the substorm events are given in Figure 2. The POLAR UV imaging data in Figure 1 is shaded for reference. Taking out the appropriate time delay of the solar wind propagation from WIND to the Earth's magnetosphere would place possible substorm triggers at 0802 UT and 0851 UT, respectively. They are indicated by arrows in the Figure. Thus, the first substorm could have been triggered either by the sharp southward turning of B_z or by a ram pressure pulse. The second substorm expansion phases onset has no obvious trigger.

The southward turning of B_z at 0802 UT was an unusual feature of the magnetic cloud. This rotation in the field towards a southwardly direction altered the storm recovery and led to a second D_{ST} intensification.

Magnetic Storms Without Substorm Expansion Phases.

An example of a magnetic storm without classical substorm expansion phases is shown in Figure 3. The magnetic cloud is indicated in panel 2, above the magnetic field magnitude and B_z panels. The available UV imaging is indicated by shading. From the bottom panel (the D_{ST} values), imaging is available during 6 hr of the storm's main phase.

Although 3 min time resolution images were available, images every ~ 12 min are shown in Figure 4 for brevity (The ~ 3 min resolution images were examined throughout the ~ 6 hr interval to look for evidence of substorm onsets. None were found within the 6 hr). The images from 1332:15 UT to 1533:00 UT (at the maximum B_s) show a double band of aurora, one centered at 62° - 65° MLAT and another centered at 70° - 72° MLAT. A good example of these double bands is found in the images of 1511:00 UT. The double bands exist primarily in the premidnight sector. The bands are not continuous, but are composed of "patches" that are typically smaller than 1 hr LT and have a poleward extent of ~ 5° latitude. The duration of the patches are ~3-5 min. When a patch from the equatorward band extends into the poleward band, these aurora have the form of "torches", noted earlier by Akasofu (1974). Similar double auroral bands and north-south aligned connecting patches have recently been discussed by Sergeev et al. (1999).

From 1522:02 UT onward, the aurora becomes quieter and was primarily single-banded. An auroral loop is found on the postmidnight sector at 1735:44 UT.

Figure 5 is another example of a magnetic storm caused by magnetic cloud B_s fields. This event occurred on February 10, 1997. The available POLAR UV imaging data is again indicated by the shading. It should be noted that this imaging is available for almost 6 hour during the storm main phase. The peak $|B|$ of ~ 8 nT and peak B_s of 8 nT occurred at ~ 1100 UT, close to the interval of peak D_{ST} (1100-1130 UT). The IMF B_s profile was smooth with very little variations.

The corresponding auroras for the entire shaded interval of Figure 5 is shown in Figure 6. The time interval between images is ~ 6 min (3 min data are available, but not shown to save space). At 0722:28 UT, the brightest UV aurora occurs on the premidnight site at $\sim 70^\circ$ latitude from 18 to 22 LT. At 0753:08 UT, an intense bright spot appears at $\sim 70^\circ$ latitude and ~ 21 LT. With time, the spot expands equatorward until it spans from 65° to 70° latitude at 0829:56 UT. The spot disappears by 0848:20 UT and there is patchy auroras from 18 to 05 LT at 65° latitude. At 0909:48 UT, the aurora again changes in a subtle way. A new "spot" forms at $\sim 70^\circ$ and ~ 19 LT. By 1023:24 UT the aurora again becomes similar to that at the beginning of this sequence: bright, high latitude aurora in the premidnight sector (~ 15 - 20 LT at $\sim 70^\circ$ latitude) and a fainter aurora from ~ 21 LT through ~ 06 LT at lower latitudes ($\sim 60^\circ$ - 70°). The "break" between these two types of aurora forms occurs at ~ 21 LT.

Poleward-aligned, small patchy forms are again found in the midnight sector. Examples can be seen in the images at 0854:28 UT and 1203:59 UT. These are similar (but less apparent), than the features shown in Figure 4.

Of the 11 storm events, 5 of them did not show evidence of substorms for the intervals that UV imaging data were available. These 5 events are listed in Table 2. The peak B_s , the duration of the strong southward field and the solar wind velocity during the B_s events are listed in columns 3, 5 and 2, respectively. The interplanetary electric field is calculated and listed in column 4.

Table 2. The 5 magnetic storms without substorm expansion phases

Event	V_{sw} (km/s)	B_s (nT)	E_{sw} (mV/m)	τ (hr)	N (cm^{-3})	G-T Intp. Criteria	D_{ST} (nT)	D_{ST}^* (nT)
1	450	11-15	>5.0	4.5	7	Y	-78	-82
2	425	7	3.0	7.0	<1	N	-68	-57
5	390	8	3.1	3.3	3	N	-84	-78
6	360	11	4.0	6.0	8	N	-45	-45
7	470	13	6.1	3.0	5	Y	-49	-50

Gonzalez and Tsurutani (1987) had determined that for the 1978-1979 solar maximum era, there was a one-to-one correspondence between interplanetary events where the electric field was $E > 5$ mV/m and $\tau > 3$ hr, and storm intensities $D_{ST} \leq -100$ nT. Every electric field event with those properties created a storm with intensity $D_{ST} \leq -100$ nT, and vice versa, large major storms with $D_{ST} \leq -100$ nT had the above electric field minimum values. This criterion also held for the following 11-year solar cycle as well. However, in Table 2, two events, 1 and 7, fit the interplanetary electric field criteria, but the storm intensities falls quite short of the $D_{ST} \leq -100$ nT intensities found earlier. One possible explanation is that storms without classical substorm expansion phases could have lower intensities.

CONCLUSIONS

We find that contrary to popular belief, there are magnetic storms that occur with an absence of "classical substorm expansion phases" (at this time we cannot say that the entire storm main phase did not have any substorm expansion phases, but we have shown two examples of ~6 hour intervals of storm main phases without "classical" substorm expansion phases). Such magnetic storms are characterized by small polewardly aligned patches, ~ 1 hr in LT, ~ 5° in latitude with durations of 3 to 5 min.

North-south elongated patches were a common features these magnetic storm auroras. Nakamura et al. (1993) have discussed similar north-south structures during active periods. Sergeev et al. (1999) has shown that bright spots in the poleward part of the double oval migrate equatorward and sometimes connect to the equatorward oval. ~ 100 keV narrow band (< 1hr in MLT), transient (1-2 min) particle injections are detected at geosynchronous orbit in relation to the auroral spots. These have been interpreted as bursty bulk flows (Baumjohann et al, 1990; Angelopoulos et al., 1992; 1995). Sandholt and Farrugia (2001) have demonstrated a one-to-one correspondence between 5-20 keV electron injections and auroral events detected in the POLAR UV images. The patch durations were ~ 2 min. Thus, bursty bulk flows may be the main process of plasma injection during magnetic cloud driven magnetic of storms.

The storms without substorm expansion phases appear to be of lower intensity then expected from previous results. It may be possible that the oxygen content in the ring current is lower due

to the lack of such expansion phases. Clearly the ring current composition should be analyzed for storms of these types.

FINAL COMMENTS

It is possible that substorm expansion phases are indeed occurring during all of these magnetic cloud induced storms (Akasofu, personal communications, 2001). Many features of substorm expansion phases are present. However, clear indications of the "classical" substorm expansion phase such as arc brightening and expansion are difficult, if not impossible to find.

Acknowledgements: Portions of this research were performed at the Jet Propulsion Laboratory, California Institute of Technology under contract with NASA.

References

- Akasofu, S.-I., The development of the auroral substorm, *Planet. Space Sci.*, *12*, 273, 1964.
- Akasofu, S.-I., A study of auroral display photographed from the DMSP-2 satellite and from the Alaska meridian chain of stations, *Space Sci. Rev.*, *16*, 617, 1974.
- Angelopoulos, V., W. Baumjohanm, C.F. Kennel, et al., Bursty bulk flows in the inner central plasma sheet, *J. Geophys. Res.*, *97*, 4027, 1992.
- Angelopoulos, V., T.D. Phan, D.E. Larson, et al., Magnetotail flow bursts: Association to global magnetospheric circulation, relationship to ionospheric activity and direct evidence for localization, *Geophys. Res. Lett.*, *24*, 2271, 1997.
- Baumjohann, W., G. Paschmann, and H. Luhr, Characteristics of high-speed flows in the plasma sheet, *J. Geophys. Res.*, *95*, 3801, 1990.
- Gonzalez, W.D., and B.T. Tsurutani, Criteria of interplanetary parameters causing intense magnetic storms ($Dst < -100$ nT), *Planet. Space Sci.*, *35*, 1101, 1987.
- Kamide, Y., W. Baumjohann, I.A. Daglis, et al., Current understanding of magnetic storms: Storm-substorm relationships, *J. Geophys. Res.*, *103*, 17705, 1998.
- Lepping, R.P., M.H. Acuna, L.F. Burlaga, W.M. Farrell, J.A. Slavin, K.H. Schatten, F. Mariani, N.F. Ness, F.M. Neubauer, Y.C. Whang, J.B. Byrnes, R.S. Kennon, P.V. Panetta, J. Scheiffle, and E.M. Worley, The WIND magnetic field investigation, *Space Sci. Rev.*, *71*, 207, 1995.
- Lepping, R.P., Private communication, 2001.
- Lyons, L.R., G.T. Blanchard, J.C. Samson, R.P. Lepping, T. Yamamoto, and T. Moretto, Coordinated observations demonstrating external substorm triggering, *J. Geophys. Res.*, *102*, 27039, 1997.

- McPherron, R.L., The role of substorms in the generation of magnetic storms, in *Magnetic Storm*, edited by B. Tsurutani et al., AGU Monograph, 98, 131, 1997.
- Nakamura, R., T. Oguti, T. Yamamoto, and S. Kokubun, Equatorward and poleward expansion of the auroras during auroral substorms, *J. Geophys. Res.*, 98, 5743, 1993.
- Ogilvie, K.W., D.J. Chornay, R.J. Fritzenreiter, F. Hunsaker, J. Keller, J. Lobell, G. Miller, J.D. Scudder, E.C. Sittler, Jr., R.B. Torbert, D. Bodet, G. Needell, A.J. Lazarus, J.T. Steinberg, J.H. Tappan, A. Mavertic, and E. Gergin, SWE, A comprehensive plasma instrument for the WIND spacecraft, *Space Sci. Rev.*, 71, 55, 1995.
- Rostoker, G., E. Friedrid, and M. Dobbs, Physics of magnetic storms in *Magnetic Storm*, edited by B. Tsurutani et al., AGU Monograph, 98, 149, 1997.
- Sandholt, P.E., and C.I. Farrugia, Multipoint observations of substorm intensifications: The high-latitude aurora and electron injections in the inner equatorial plasmashet, *Geophys. Res. Lett.*, 28, 483, 2001.
- Sergeev, V.A., K. Liou, C.-I. Meng, P.T. Newell, M. Brittnacher, G. Parks, and G.D. Reeves., Development of auroral streamers in association with localized injections to the inner magnetotail, *Geophys. Res., Lett.*, 26, 417, 1999.
- Tsurutani, B.T. and W.D. Gonzalez, The interplanetary causes of magnetic storms: A review, in *Magnetic Storm*, edited by B. Tsurutani et al., AGU Monograph, 98, 77, 1997.

FIGURE CAPTIONS

Figure 1. Two substorms detected in the POLAR UV images.

Figure 2. Interplanetary magnetic cloud events and resultant geomagnetic activity. The times of two substorms shown in Figure 1 (with suitable time shifts) are indicated.

Figure 3. A magnetic cloud event causing a magnetic storm. The interval of POLAR UV images is designated by shading. There are no substorm expansion phases within the ~ 6 hr of imaging data.

Figure 4. Imaging data for the shaded region of Figure 3.

Figure 5. A storm event on February 10, 1997. The figure uses the same format as Figure 3.

Figure 6. POLAR UVI data for the shaded region of Figure 5.

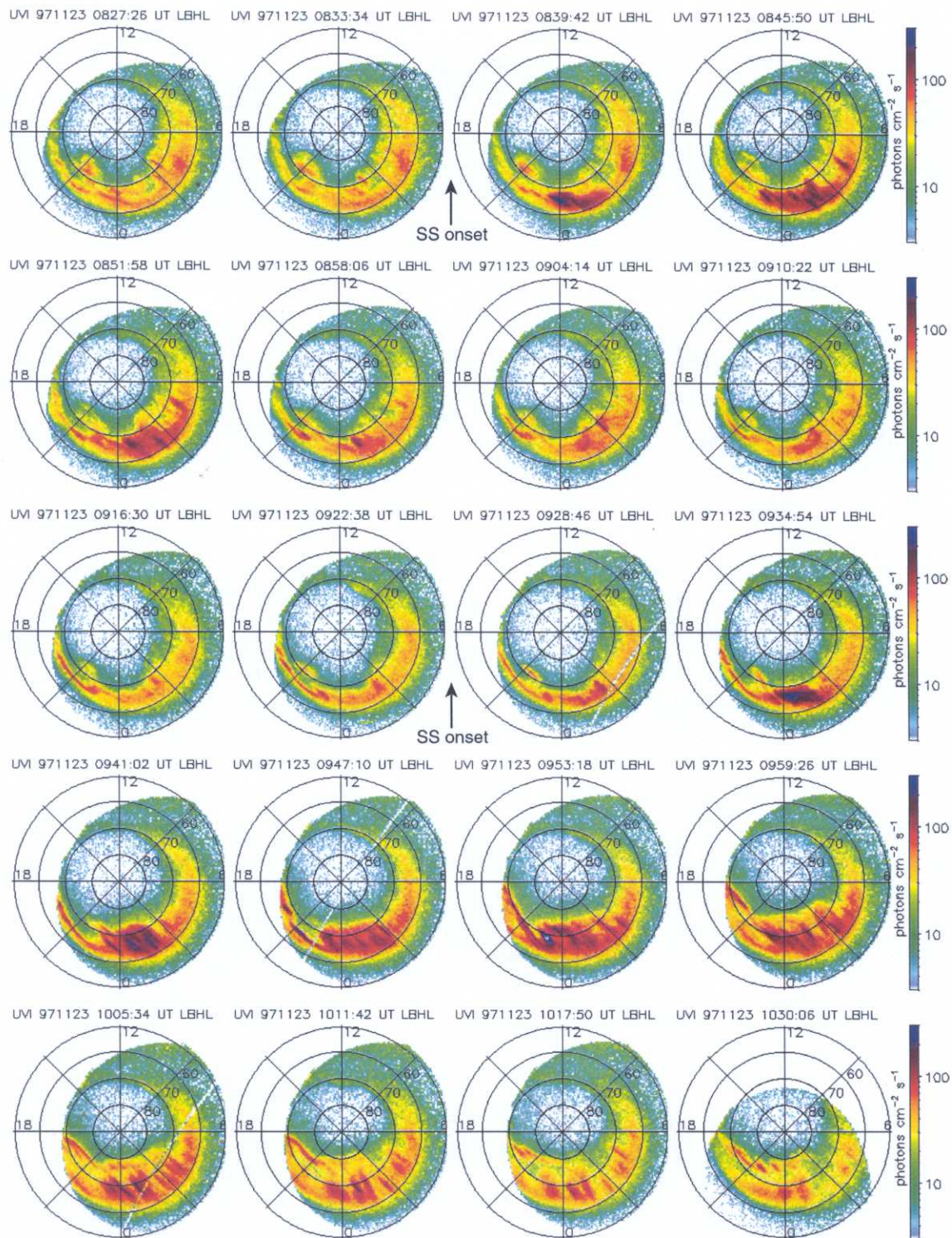


Figure 1

WIND solar wind data and geomagnetic AE and Dst for 11/23/1997

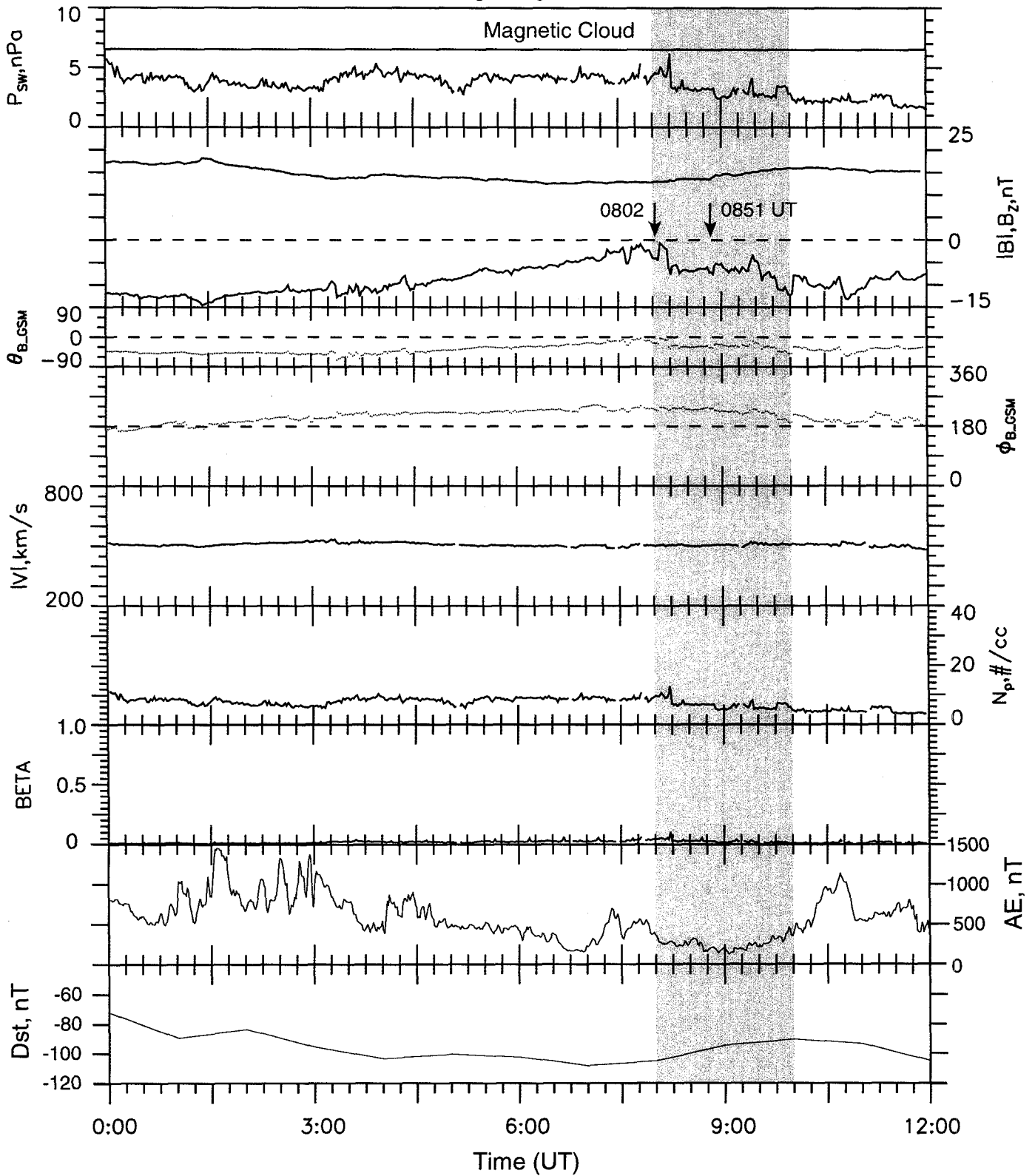


Fig 2

WIND solar wind data and geomagnetic AE and Dst for 7/15/1997

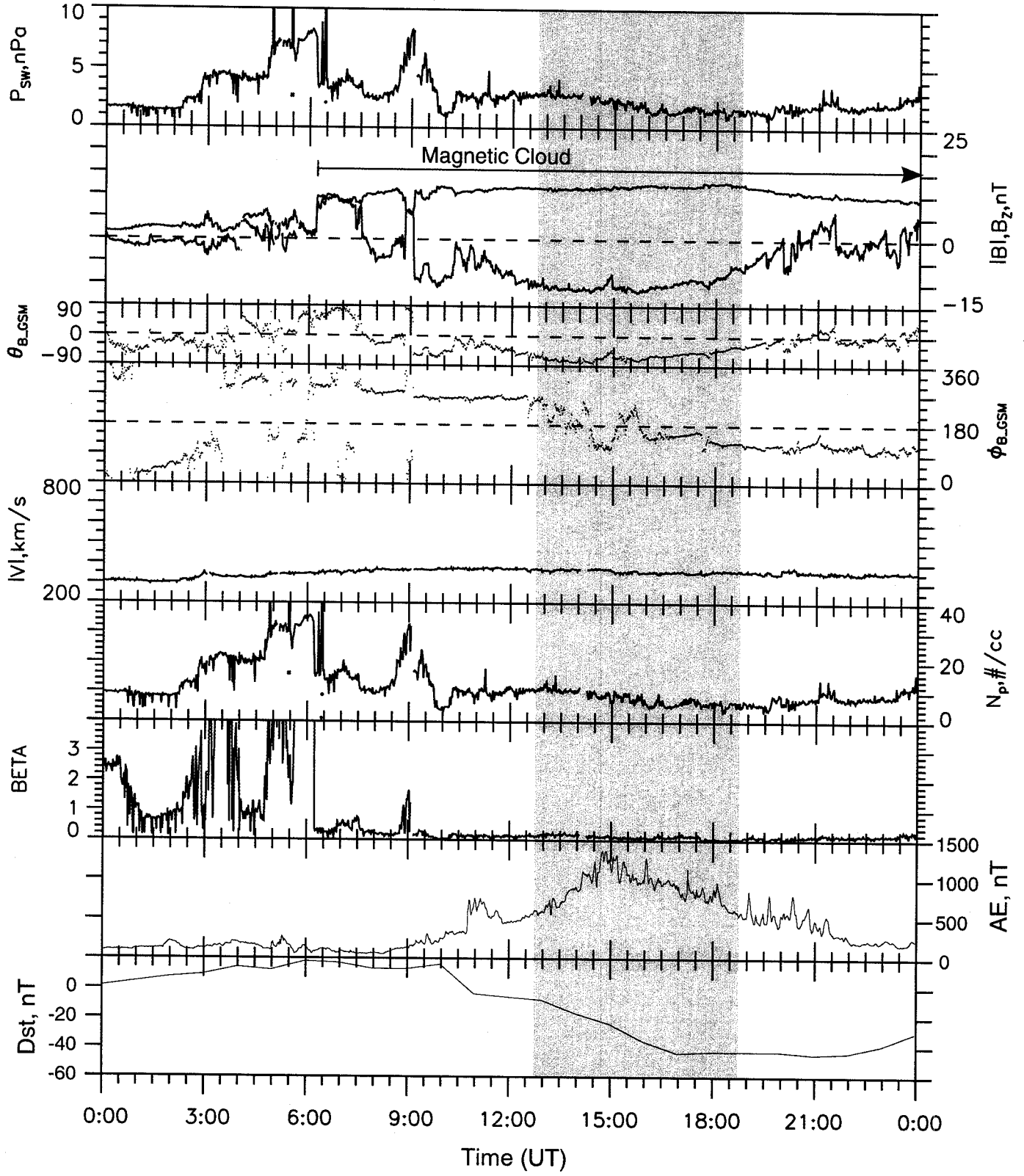


Figure 3

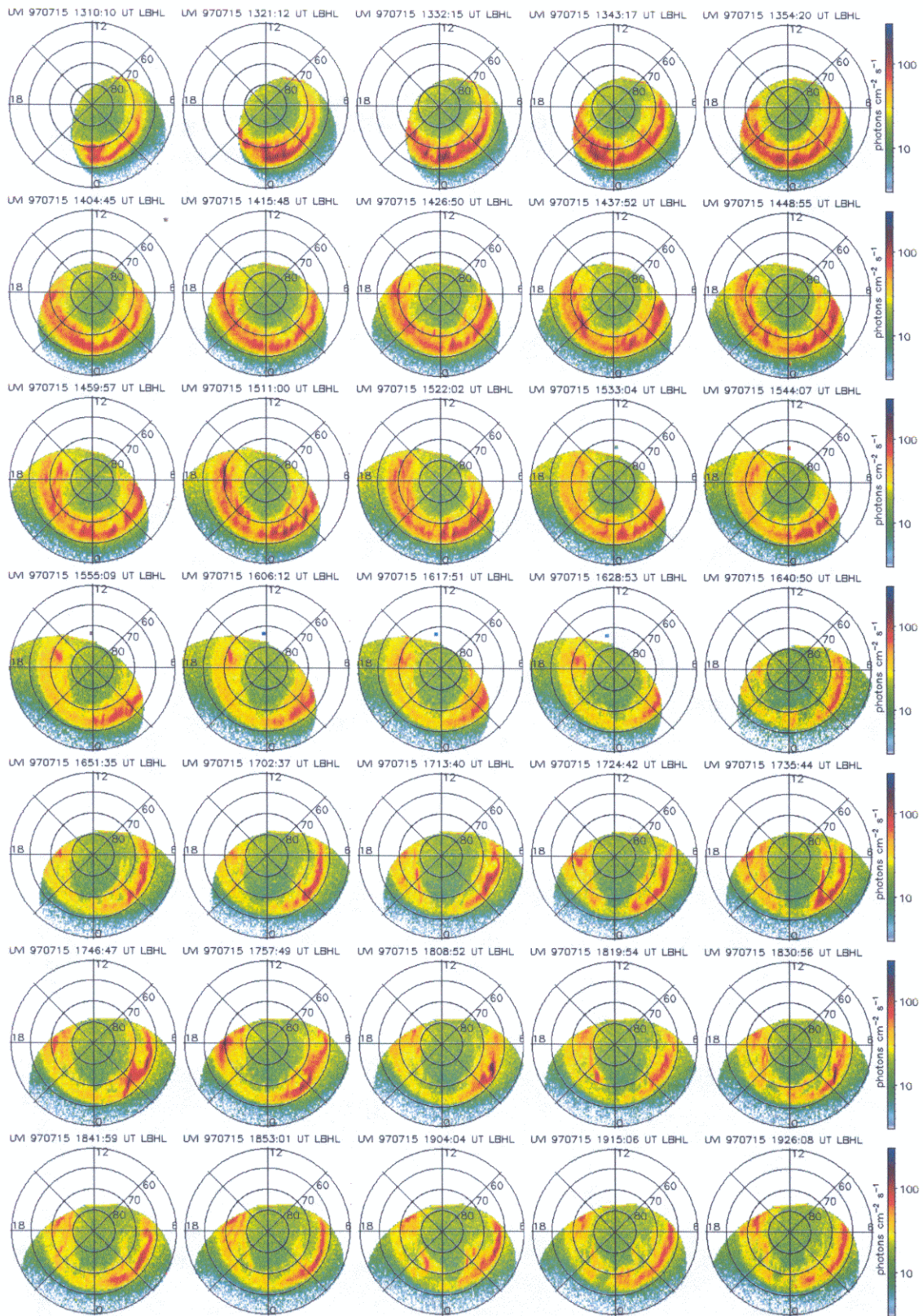


Figure 4

WIND solar wind data and geomagnetic AE and Dst for 2/10/1997

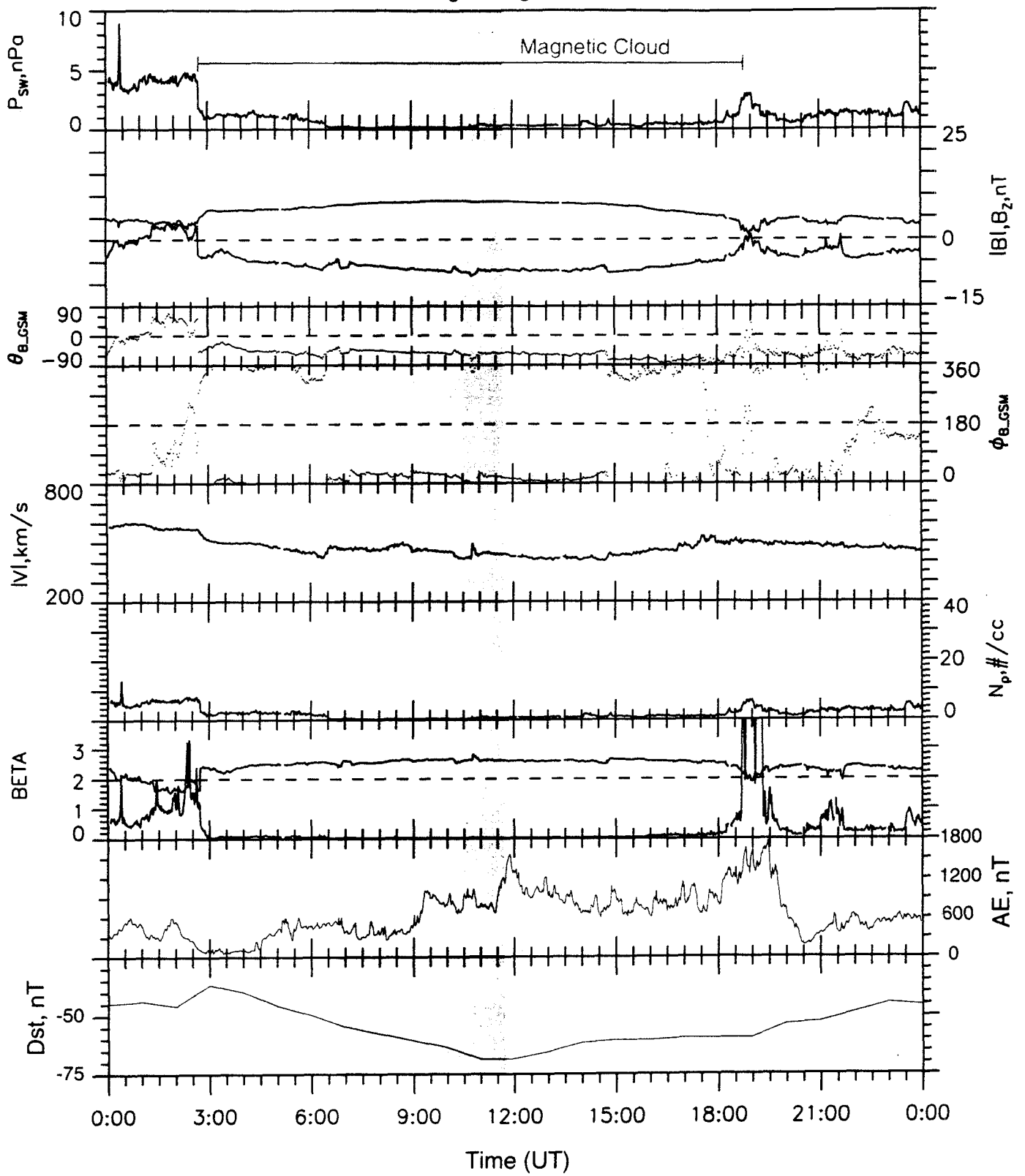


Figure 5

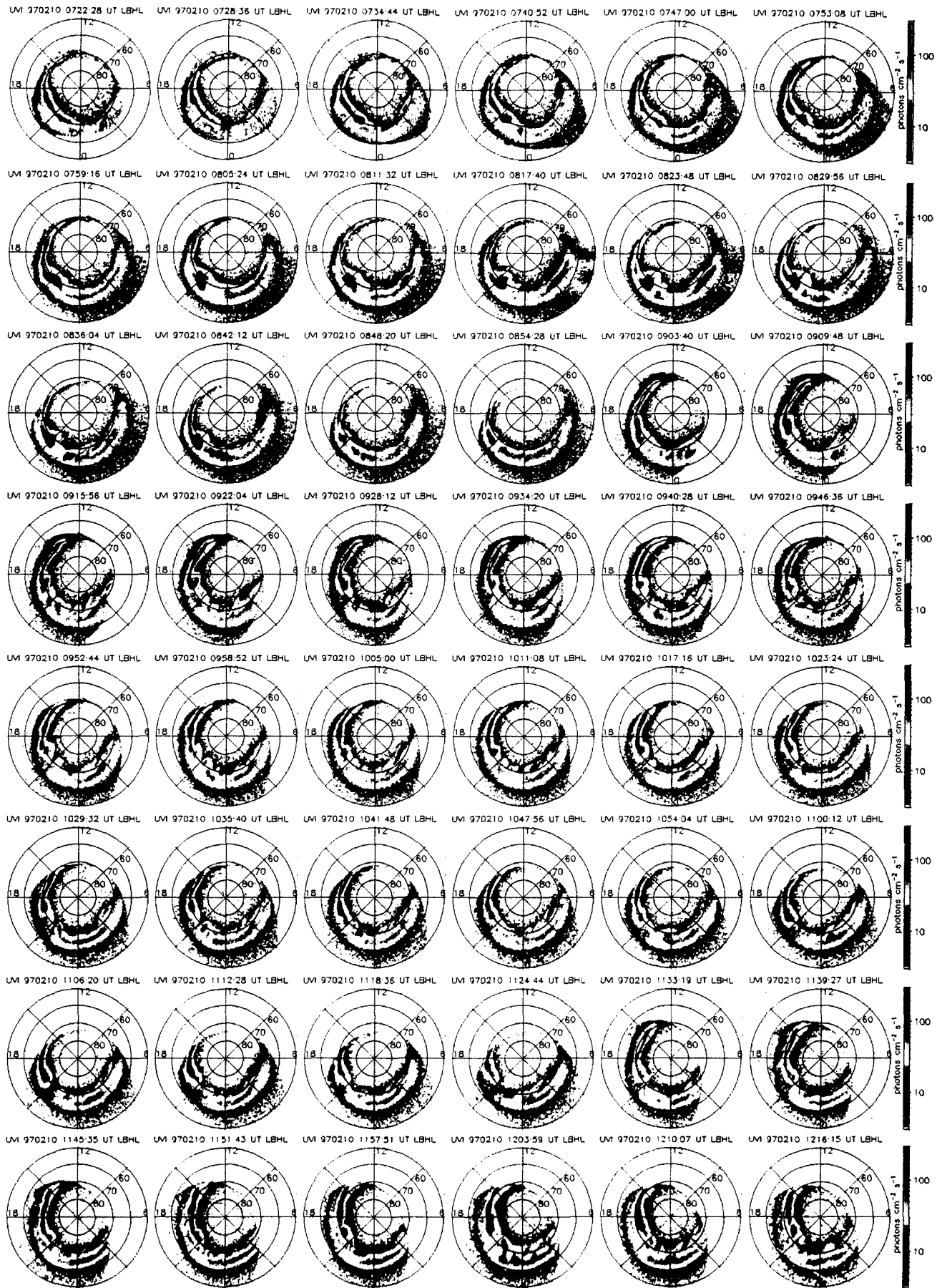


Figure 6